

An Improved Weighted Distance Scheme for ART for Cone-beam CT [★]

Huihua KONG^{1,2}, Jinxiao PAN^{1,2,*}, Yan HAN²

¹*School of Science, North University of China, Taiyuan 030051, China*

²*National Key Laboratory for Electronic Measurement Technology, North University of China, Taiyuan 030051, China*

Abstract

Iterative methods for image reconstruction such as algebraic reconstruction techniques (ART) are more robust and flexible than analytical inversion methods in handling incomplete, noisy, and dynamic data. The major disadvantage of the iterative methods is their slow computational speed, especially for cone-beam CT. In ART, the convergence speed heavily depends on the order in which the projections are accessed. The methods for choosing the order of the projections for parallel and fan beams have been proposed in previous studies. The Weighted Distance Scheme (WDS) which optimizes the selection in a global sense and takes the projection selection into consideration at iteration boundaries. However, the WDS is only adapted to the cases in which the projection views are distributed uniformly in angle $[0, \pi)$. To improve the convergence speed of the ART for cone-beam CT, an improved WDS (IWDS) which extends the applying scale of the WDS from uniform projection sampling in $[0, \pi)$ to uniform and non-uniform projection sampling in $[0, 2\pi)$ is proposed in this study. The new method is evaluated and compared with traditional projection access schemes for circular cone-beam x-ray computed tomography reconstruction. Experiments show that IWDS can accelerate the convergence of the reconstruction algorithm and produce more accurate images.

Keywords: Image Reconstruction; Projection Order; WDS

1 Introduction

Cone-beam x-ray computed tomography (CT) has two major categories of image reconstruction: analytic methods and iterative methods. Iterative methods such as algebraic reconstruction techniques (ART) [1] and expectation maximization (EM) [2, 3] are inherently more robust to noise and truncation of the projections than analytic inversion methods [4, 5].

*Project supported by the the 973 program (No. 2011CB311804), SRFDP (2012142011006) TSTIT, and the National Science Foundation of China (No. 61227003, 61171179, 11247244 and 61071193) and the Science Foundation of Shanxi Province (No. 2010011002-1, 2010011002-2 and 2012021011-2).

*Corresponding author.

Email address: huihuak@163.com (Jinxiao PAN).

The ART was originally proposed by Kaczmarz in 1937 [6] and was first published for CT by Gordon et al in 1970 [1]. Because ART applies only one ray to update the entire image at each step, the order in which the collected data are accessed during the reconstruction procedure has great impact on this algorithm's convergence speed.

Several observations have been made on the improvements of the projection access systems. However even now, there is no gold standard in this branch of tomography. Generally speaking, Random Access Scheme (RAS) [7], Prime Number Decomposition (PND) principle [8], Multilevel Access Scheme (MLS) [9], Weighted Distance Scheme (WDS) [10] and Golden ratio-based (GR) ordering [11] are considered effective ordering.

Among the existing projection access systems, the MLS is only adapted to the case that the projections uniformly distributed in angle $[0, \pi)$. Though the PND can be applied to the angle $[0, \pi)$ or $[0, 2\pi)$, it is also only adapted to the uniformly distributed projections and it requires that the projection views number be non-prime. The GR can also be applied to the angle $[0, \pi)$ or $[0, 2\pi)$, however this method leads the non-uniformed projection distribution and it is difficult to apply this method to the given non-uniformed projection views. The WDS optimizes the selection in a global sense and considers the projection selection at iteration boundaries, however, it is only applicable to the case that the projections distributed uniformly in the angle $[0, \pi)$. Compared with the four systems, the RAS can be applied in any angle interval, and its extension to non-uniform projection views is straightforward. The aim of this paper is to extend the WDS to the case of uniform and non-uniform projection sampled in the interval $[0, 2\pi)$ and evaluate the improved WDS (IWDS) versus the sequential access (SAS) and RAS for cone-beam x-ray computed tomography reconstruction, for the case of circular acquisition.

Andersen and Kak showed that the quality of the reconstruction could be significantly improved if the image is updated using per projection image instead of projection ray [12]. Further more, Guan and Gordon concluded that reordering the rays in each view would have little effect on the convergence performance [9]. So the analysis of the new projection ordering scheme is performed using simultaneous ART (SART), in which all ray in a given projection are calculated and used for each update step.

This paper is organized as follows. A brief review of SART is given in Section 2. The WDS and the proposed IWDS are introduced in Section 3. Section 4 describes the experiments, quantitative evaluation metric, and the results. The conclusion is given in Section 5.

2 Reconstruction Algorithm

The image reconstruction problem in CT can be modeled by the following equation

$$AX = Y, \quad (1)$$

where $Y = (y_i)_{I \times 1} \in \mathbb{R}^I$ is the projection data, $X = (x_j)_{J \times 1} \in \mathbb{R}^J$ is the image vector, and $A = (a_{ij})_{I \times J}$ is the projection matrix, a_{ij} is the length of the intersection of the j -th voxel with projection ray i . Most of the voxels are not traversed by ray i , so A is quite sparse. The problem is to reconstruct the X from the Y . A direct solution might be infeasible, because of the ill-conditioning problem.

The SART algorithm provides an efficient iterative way to solve the linear systems of Eq. (1).

It can be written as

$$x_j^{(k+1)} = x_j^{(k)} + \lambda_k \cdot \frac{1}{\sum_{i \in P_l} a_{ij}} \sum_{i \in P_l} \frac{y_i - \sum_{j=1}^J a_{ij} x_j^{(k)}}{\sum_{j=1}^J a_{ij}} \cdot a_{ij}, \tag{2}$$

where λ_k is the relaxation parameter and P_l is the projection image at $(l + 1)$ -th view.

Since the SART is proposed in 1984 [12], it remains a powerful tool for iterative reconstruction and has been used a number of studies with impressive results [13–17].

3 Projection Ordering Systems

3.1 Weighted distance scheme

In 1997, Klaus Mueller proposed a globally optimizing projection ordering method for ART, i.e., WDS. The WDS optimizes the angular distance of a newly selected projection with respect to the complete sequence of all previously applied projections and guarantees a smooth transition between iterations.

In the WDS, the projection views $[P_0, P_1, \dots, P_{M-1}]$ are assumed to be distributed uniformly in the interval $[0, \pi)$ by an angle $\varphi = \pi/M$, where M is the total number of the projection views.

All projection views are first stored in set Λ , and the newly selected projection will be stored one by one in a circular queue Θ . When a projection P_i is selected from Λ , it is removed from Λ and inserted into Θ . Usually, the first element of Θ is the projection at orientation angle $\varphi = 0$, i.e. P_0 . The length S of queue Θ means a projection’s influential power fades to zero after S more projections have been selected. In this paper, the length S equals M . Let Q denote the number of projections currently in Θ . If $Q < S$, subsequently used projections are added to consecutive positions in Θ . If $Q = S$, the oldest projection in Θ is overwritten by the newly selected projection and ceases to influence the selection process.

The weighted mean of the repulsive forces acting on a projection P_l , denoted by μ_l , is given by

$$\mu_l = \frac{\sum_{q=0}^{Q-1} w_q (\frac{S}{2} - d_{lq})}{\sum_{q=0}^{Q-1} w_q}, \tag{3}$$

where $d_{lq} = \min(|l - q|, S - |l - q|)$ denoting the minimal distance of two projections P_l and P_q , and a weight factor $w_q = (q + 1)/Q$ ensures that projections applied more recently have a stronger repulsive effect than the projections applied earlier in the reconstruction procedure.

The weighted standard deviation of the distances d_{lq} , denoted by σ_l , is given by

$$\sigma_l = \sqrt{\frac{\sum_{q=0}^{Q-1} w_q (d_{lq} - \bar{d}_l)^2}{\sum_{q=0}^{Q-1} w_q}}, \tag{4}$$

where $\bar{d}_l = \frac{\sum d_{lq}}{Q}$. Maintaining a small σ_l of the projection distances prevents projections from clustering into groups of angular viewing ranges.

Finally, μ_l and σ_l are normalized to a range of $[0, 1]$, by

$$\tilde{\mu}_l = \frac{\mu_l - \min_{k \in \Lambda}(\mu_k)}{\max_{k \in \Lambda}(\mu_k) - \min_{k \in \Lambda}(\mu_k)}, \tag{5}$$

$$\tilde{\sigma}_l = \frac{\sigma_l - \min_{k \in \Lambda}(\sigma_k)}{\max_{k \in \Lambda}(\sigma_k) - \min_{k \in \Lambda}(\sigma_k)}, \tag{6}$$

The objective function used to select the next projection from Λ is defined as

$$D_l = \tilde{\sigma}_l^2 + 0.5 \cdot \tilde{\sigma}_l^2, \tag{7}$$

then, the next projection selected from Λ should satisfy

$$\min_{l \in \Lambda}(D_l), \tag{8}$$

3.2 Improved WDS

One contribution of this paper is to extend the using range of the WDS from $[0, \pi)$ to $[0, 2\pi)$ and from uniform projection to non-uniform projection distributions. In the following, we firstly explain the concepts of uniform projection and non-uniform projection distributions.

Supposing the projections $[P_0, P_1, \dots, P_{M-1}]$ are sampled in the interval $[0, 2\pi)$, let

$$\Delta\varphi_i = \text{radian}(P_{i+1}) - \text{radian}(P_i), \quad (0 \leq i \leq M - 2), \quad \Delta\varphi_{M-1} = 2\pi - \text{radian}(P_{M-1}) \tag{9}$$

where $\text{radian}(P_i)$ is the orientation angle of the projection view P_i .

If $\Delta\varphi_i(0 \leq i \leq M - 1)$ all equal, namely,

$$\Delta\varphi_0 = \Delta\varphi_1 = \dots = \Delta\varphi_{M-2} = \Delta\varphi_{M-1}, \tag{10}$$

then the projections are distributed uniformly in $[0, 2\pi)$.

If not all $\Delta\varphi_i(0 \leq i \leq M - 1)$ equal, then the projections are distributed non-uniformly in $[0, 2\pi)$.

A graph showing a sketch of the uniform and non-uniform projection distributions sampling in $[0, 2\pi)$ is given in Fig. 1.

In the original WDS, the projections are assumed to be distributed uniformly in the interval $[0, \pi)$. So the minimal distance of two projections P_l and P_q can be computed by the difference of the index of the projections. However, it is illogical when the projection views are distributed non-uniformly. From Fig. 1(b), we see the geometric position of one projection can be denoted by the orientation angle of this projection. So the minimal distance d_{lq} between the two projections is redefined as the acute angle between the direction of two projection

$$d_{lq} = \begin{cases} |r_l - r_q|, & 0 \leq |r_l - r_q| < \frac{\pi}{2}, \\ \pi - |r_l - r_q|, & \frac{\pi}{2} \leq |r_l - r_q| < \pi, \\ |r_l - r_q| - \pi, & \pi \leq |r_l - r_q| < \frac{3\pi}{2}, \\ 2\pi - |r_l - r_q|, & \frac{3\pi}{2} \leq |r_l - r_q| < 2\pi, \end{cases} \tag{11}$$

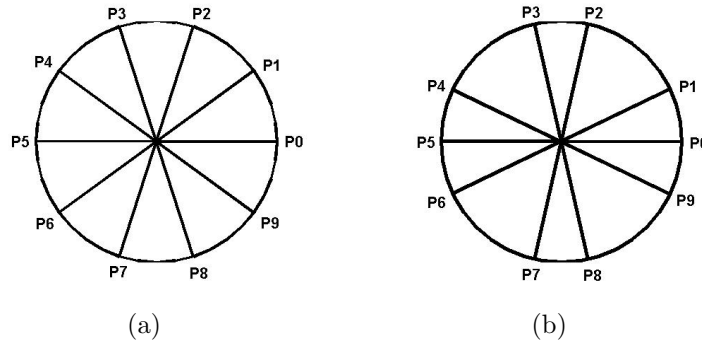


Fig. 1: The sketch map of (a) uniform projection and (b) non-uniform projection distributions sampling in $[0, 2\pi)$

where r_l and r_q denotes the orientation angle of the projection views P_l and P_q , respectively, $l, q = 0, 1, \dots, M - 1$.

Because a larger spacing of two projections results in a smaller repulsive force, the weighted mean μ_l of the repulsive forces acting on a projection P_l is redefined as

$$\mu_l = \sum_{q=0}^{Q-1} \omega_q \cos(d_{lq}), q \in \Theta, l \in \Lambda, \tag{12}$$

where $\omega_q = \frac{(q+1)}{\sum_{i=0}^Q i} = \frac{w_q}{\sum_{q=0}^{Q-1} w_q}$, which is similar to w_q . A small cosine of the radian difference between the two projections means a large space of two projections.

The weighted standard deviation of the distances d_{lq} is

$$\sigma_l = \sqrt{\sum_{l=0}^{Q-1} w_q (d_{lq} - \bar{d}_l)^2}, q \in \Theta, l \in \Lambda, \tag{13}$$

where $\bar{d}_l = \frac{\sum d_{lq}}{Q}$.

Then, the next projection view selected from Λ should still satisfy:

$$\min_{l \in \Lambda} (D_l) = 0.5 \cdot \tilde{\mu}_l^2 + 0.5 \cdot \tilde{\sigma}_l^2, \tag{14}$$

The computation for $\tilde{\mu}_l$ and $\tilde{\sigma}_l$ is same as (5), (6). Experiments indicate that a factor of 0.5 to weigh $\tilde{\mu}_l^2$ and $\tilde{\sigma}_l^2$ yields ideal results for cone-beam x-ray CT reconstruction for the case of circular acquisition.

The projections are distributed in $[0, 2\pi)$, making it possible that there are two projections in Λ satisfying (14) simultaneously, for example, in Fig. 1(a), projections P_3 and P_8 could satisfy (14) at the same time. Considering that selected projections should be distributed as uniformly as possible, the next projection should satisfy minimizing the asymmetry of the radian of the elements in Θ , i.e.,

$$\min_{i=1,2} |skewness(r_{\Theta[1]}, r_{\Theta[2]}, \dots, r_{\Theta[Q]}, r_{k[i]})|, \tag{15}$$

where $r_{\Theta[j]}$ denotes the radian of j -th element in Θ , and $r_{k[i]}$ denotes the radian of projection k_i .

The proposed method can be applied to angle $[0, 2\pi)$ by adding an objective function (15) and can be applied to non-uniform projections by modifying the minimal distance d_{lq} between the two projections.

4 Simulation Study

The 3D $128 \times 128 \times 128$ voxels Shepp-Logan model is selected as the test model. Considering that PND and GR are difficult to be modified for dealing with the given non-uniform projection sampling, in the experiments, we compare IWDS with SAS and RAS.

To verify the validity of IWDS, two sets of experiments are conducted to implement the comparative studies. In the first experiment, 360 projection views are distributed uniformly in angle $[0, 2\pi)$. In the second experiment, 210 projection views are distributed non-uniformly in angle $[0, 2\pi)$, in which the angle interval between the two projections is 1.5° in $[0, \pi)$ and 2° in $[\pi, 2\pi)$ respectively.

We use a circular orbit to acquire the projection views $[P_0, P_1, \dots, P_{M-1}]$. The detector plane contains 160×160 detection channels. The distance from source to detector plane equals to 1,000 pixels and the distance from source to centre of rotation equals to 700 pixels. To eliminate the effects of another variable in the comparative process, we used a fixed value of $\lambda_k = 0.3$ throughout the reconstruction procedure.

In order to compare IWDS with other ordering systems, the normalized mean square error (NRMSE)

$$NRMSE = \sqrt{\frac{\sum_{i=1}^J (x_i - \hat{x}_i)^2}{\sum_{i=1}^J (x_i - \bar{x})^2}} \quad (16)$$

is calculated, where x_i refers to the i -th voxel value in the true image, \hat{x}_i represents the value of voxel i in the reconstructed image and \bar{x} represents the image average value in the true image. This measure quantifies the overall difference between the reconstructed image and the true image, and can be used to evaluate the convergence rate of the algorithm.

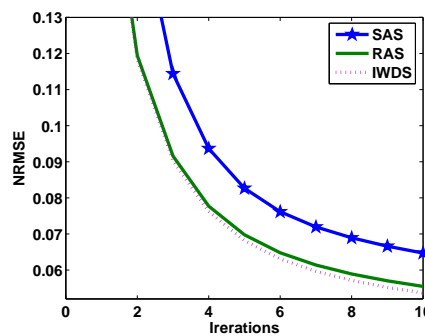


Fig. 2: The NRMSE as a function of iterations for uniform projection distributions

Fig. 2 gives the plots of the NRMSE as a function of the iteration number when the 360 projection views are distributed uniformly in angle $[0, 2\pi)$. Clearly, SAS yields larger NRMSE

than other two orders at any number of iterations and IWDS is slightly superior to RAS in convergence speed. It implies that reasonable adjustment of the projection views can accelerate the speed of the reconstruction.

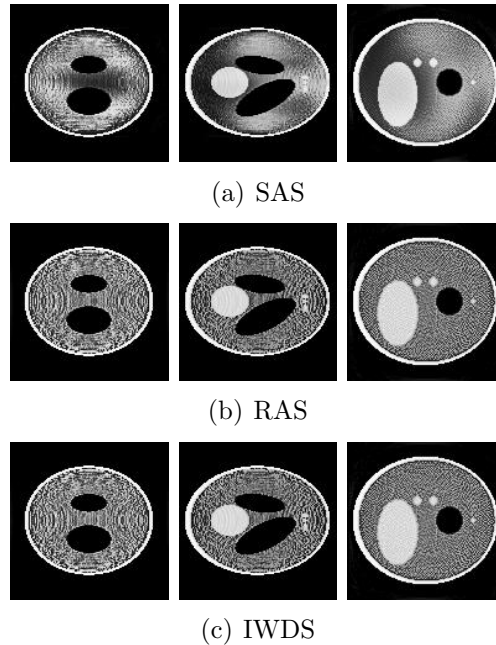


Fig. 3: Reconstruction results at the central location of three different axes after two iterations for uniform projection distributions

The three central slices of the reconstruction after two iterations using the three projection ordering schemes are shown in Fig. 3. The graph clearly shows the quality of the image reconstructed by SAS is worse than that reconstructed by RAS and IWDS, since there are some visible low-frequency artifacts in Fig. 3(a).

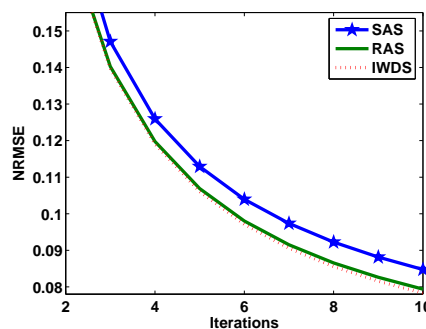


Fig. 4: The NRMSE as a function of iterations for non-uniform projections sampling in angle $[0, 2\pi]$

The NRMSE and the images reconstructed from non-uniform projection distributions are shown in Fig. 4-5. Fig. 4 shows that the IWDS method is superior to SAS and slightly excellent than RAS in the convergence speed. From Fig. 5(a), we can see there is some visible low-frequency artifact in central slices reconstructed by SAS. And the artifacts slowly decrease at higher iterations.

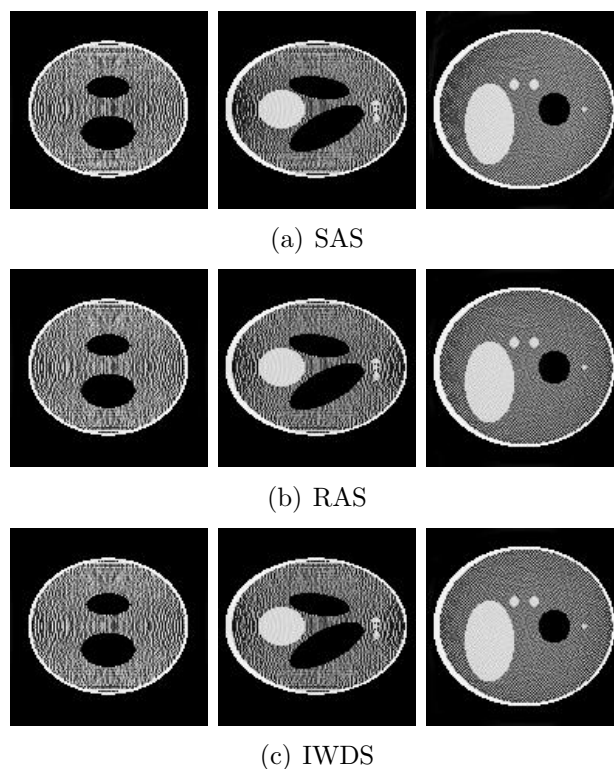


Fig. 5: Reconstruction results at the central location of three different axes after two iterations for non-uniform projection distributions

5 Conclusion

In this study, an improved WDS which extends the applying scale of the WDS is proposed. This method extends original WDS's using range from $[0, \pi)$ to $[0, 2\pi)$ and from uniform projection to non-uniform projection distributions. The validity of the new method for cone beam CT is evaluated with the 3D Shepp-Logan model by image quality comparison and numerical measures.

Compared with the three systems, RAS and IWDS can be applied to angle $[0, 2\pi)$, and are insensitive to the distribution of the projections. Furthermore, IWDS is more controllable and deterministic than RAS.

Although results have been obtained only for ART, it is anticipated that other iterative reconstruction algorithms such as OS-type methods [18-20] will act likely. And the proposed method can also be applied to spiral cone-beam CT.

References

- [1] R. Gordon, R.B. Ender, G.T. Herman. Algebraic reconstruction techniques (ART) for three-dimensional electron microscopy and X-ray photography. *J. Theoret. Biol.*, 29 (1970) 471-481.
- [2] L.A. Shepp and Y. Vardi, Maximum likelihood reconstruction in positron emission tomography, *IEEE Trans. Med. Imag.*, 1 (1982) 113-122.
- [3] K. Lange and R. Carson, EM reconstruction algorithms for emission and transmission tomography, *J. Comput. Assist. Tomogr.*, 8 (1984) 306-316.

- [4] S. H. Manglos, Truncation artefact suppression in cone-beam radionuclide transmission CT using maximum likelihood techniques: evaluation with human subjects, *Phys. Med. Biol.*, 3791992 549-562.
- [5] D. R. Gilland, R. J. Jaszczak and R. E. Coleman, Transmission CT reconstruction for offset fan beam collimation, *IEEE Trans. Nucl. Sci.*, 47 (2000) 1602-1606.
- [6] S. Kaczmarz. Angenäherte Auflösung von Systemen linearer Gleichungen, *Bull. Acad. Polon. Sci. Lett. A*, (1937) 335-357.
- [7] M.C. van Dijke, Iterative methods in image reconstruction, Ph.D. Dissertation, Rijksuniversiteit Utrecht, The Netherlands, 1992.
- [8] G.T. Herman and L.B. Meyer, Algebraic reconstruction technique can be made computationally efficient, *IEEE Trans. Med. Imag.*, 12 (1993) 600-609.
- [9] H. Guan and R. Gordon, A projection access order for speedy convergence of ART (algebraic reconstruction technique): a multilevel scheme for computed tomography, *Phys. Med. Biol.*, 39 (1994) 2005-2022.
- [10] K. Mueller, R. Yagel and F. Cornhill, The weighted distance scheme: A Globally Optimizing Projection Ordering Method for ART, *IEEE Trans. Med. Imag.* 16 (1997) 223-230.
- [11] T. Köhler, A Projection Access Scheme for Iterative Reconstruction Based on the Golden Section, in *Proc. of the 2004 IEEE Nuclear Science and Medical Imaging Conference*, CDROM M10-200, Rome, Italy, October 16-22 (2004) 3961-3965.
- [12] A. H. Andersen, and A. C. Kak, Simultaneous algebraic reconstruction technique (SART): A superior implementation of the ART algorithm, *Ultrason. Imag.*, 6 (1984) 81-94.
- [13] G. Wang, D. L. Snyder, J. A. O'Sullivan, and M. W. Vannier, Iterative deblurring for CT metal artifact reduction, *IEEE Trans. Med. Imag.*, 15 (1996) 657-664.
- [14] G. Wang, M.W. Vannier, M.W. Skinner, M.G. P. Cavalcanti, and G. Harding, Spiral CT image deblurring for cochlear implantation, *IEEE Trans. Med. Imag.*, 17 (1998) 251-262.
- [15] G. Wang, G.D. Schweiger, and M.W. Vannier, An iterative algorithm for X-ray CT fluoroscopy, *IEEE Trans. Med. Imag.*, 17 (1998) 853-856.
- [16] K. Mueller, and R. Yagel, Anti-aliased three-dimensional cone-beam reconstruction of low-contrast objects with algebraic methods, *IEEE Trans. Med. Imag.*, 18 (1999) 519-537.
- [17] K. Mueller, and R. Yagel, Fast implementations of algebraic methods for three-dimensional reconstruction from cone-beam data, *IEEE Trans. Med. Imag.*, 18 (1999) 538-548.
- [18] H.M. Hudson and R.S. Larkin, Accelerated image reconstruction using ordered subsets of projection data, *IEEE Trans. Med. Imag.*, 13 (1994) 601-609.
- [19] C. Kamphuis and F. J. Beekman, Accelerated iterative transmission CT reconstruction using an ordered subsets convex algorithm, *IEEE Trans. Med. Imag.*, vol. 17 (1998) 1101-1105.
- [20] J. S. Kole and F. J. Beekman, Evaluation of the ordered subset convex algorithm for cone-beam CT, *Phys. Med. Biol.*, 50 (2005) 613-623.